

Lawrence Livermore Laboratory Report No. UCRL-75018, 1973 (unpublished).

¹⁰M. Ablowitz, A. Newell, D. Kaup, and H. Segur,

Stud. Appl. Math. **53**, 249 (1974).

¹¹J. Satsuma and N. Yajima, Prog. Theor. Phys., Suppl. **55**, 284 (1974).

Generation of an Intense Ion Beam by a Pinched Relativistic Electron Beam

P. Gilad and Z. Zinamon

The Weizmann Institute of Science, Rehovot, Israel

(Received 17 May 1976)

The tightly pinched electron beam of a pulsed electron accelerator is used to generate an intense beam of ions. A foil anode and vacuum drift tube are used. The space-charge field of the pinched beam in the tube accelerates ions from the foil anode. Ion currents of 10 kA at a density of 5 kA/cm^2 with pulse length of 50 nsec are obtained using a 5 kJ, 450 kV, $3\text{-}\Omega$ diode.

For a possible application of ion beams to pellet fusion, high current densities of ions on the target are necessary.¹ It is therefore desirable to investigate high-current-density ion beams, both for direct application to fusion and for basic studies of the interaction of such beams with matter.

Since the discovery of ion acceleration by electron beams,² acceleration in vacuum drift tubes has been studied by several investigators.³ The reflex triode technique has been suggested by Humphries, Lee, and Sudan⁴ using either a real or virtual second cathode, and by Creedon and co-workers⁵ using a thin anode foil. Other schemes of using anodes as ion sources have also been suggested.⁶ Recently, high ion current densities were reported by Prono, Shearer, and Briggs⁷ using the planar reflex diode technique.

The focal area of a tightly pinched electron beam seems to be a promising source of high intensity ion currents. With a foil anode, a high density of electrons is expected in this region on both the diode and the drift-tube sides of the anode. The space charge on the drift tube side is expected to accelerate ions generated in the anode plasma into the drift tube. In this work an intense electron beam, tightly pinched on a foil anode, was used to generate a high-current-density ion beam. Unlike the planar reflex diode technique, no external magnetic field was applied to prevent pinching. Rather, the diode was designed to produce a tight pinch. The measurements were performed directly on the ions accelerated down the drift tube.

The type of diode used is shown in Fig. 1. The brass cathode was 80 mm in diameter and was coated with Aquadag carbon. The anode was 40-

μm -thick aluminum foil. The anode-cathode gap was 3.2 mm. The diode peak voltage was 450 kV and the peak current was 165 kA. The current rise time was 25 nsec, and the pulse width was 80 nsec. Under such conditions the beam tightly pinched, as was verified by x-ray pinhole photographs which were taken regularly. The drift tube was 15 cm in diameter, pumped down to 10^{-4} Torr. The drift-tube side of the anode was coated with 1 mg/cm^2 of CD_2 . A target made of 0.3-mm-thick copper coated with 2 mg/cm^2 of CD_2 was centered on the drift tube axis at a distance of 4.5 cm from the anode. The radii of the coated portions on the anode and target were varied in the experiments. The properties of the ion beam were studied by analyzing the neutrons generated by reactions in the target and by studying

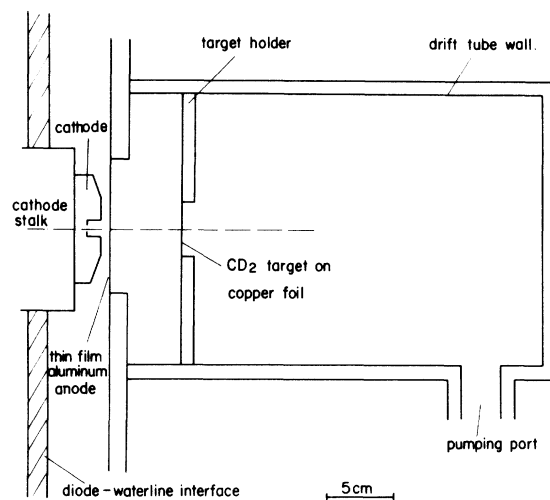


FIG. 1. Diode and target configurations for the ion acceleration experiments.

the current and beam front velocity in the drift tube.

The total number of neutrons was determined, using a silver activation counter of design similar to that of Lautner and Bannerman⁸ and calibrated at a neutron energy of 4 MeV on a Van de Graaff accelerator using the reaction $d(d, n)\text{He}^3$ from a gas target.

The incident ion energy was determined by neutron time-of-flight measurements and by the carbon foil technique. For the time-of-flight measurements, two scintillation detectors were placed at distances 60 and 500 cm from the target. Both detectors used RCA 8575 photomultiplier tubes and 2-in.-diam, $\frac{1}{2}$ -in.-thick Pilot B scintillators. In the nearer detector a neutral density filter adjusted the signal height to be similar to that of the far detector. The same voltage was applied to both photomultipliers. A typical pair of scintillation detector traces is shown in Fig. 2. The neutron time of flight was determined by the time difference between the heads of the two signals. This measurement yields a value of 500 keV for the deuteron energy.

In the carbon foil technique, 200 and 400 $\mu\text{g}/\text{cm}^2$ carbon foils were placed on the CD_2 targets to slow down the deuterons. The contribution to the neutron count by the reaction $^{12}\text{C}(d, n)^{13}\text{N}$ in the foils was measured separately and subtracted. The contribution of the same reaction in the CD_2 was estimated by taking the neutron count of a thick carbon target. This was at most 7% of the count with a bare CD_2 target, not correcting for the increased counter efficiency at low neutron energies. Considering the higher stopping power of CD_2 and the lower density of carbon there, we neglected this contribution. The contribution of

the reaction $d(^{12}\text{C}, n)^{13}\text{N}$ by possible carbon ions in the beam is nonexistent at the energies relevant here. The relative neutron counts were 1, 0.58 ± 0.05 , and 0.36 ± 0.07 in bare target and in targets covered with 200 and 400 $\mu\text{g}/\text{cm}^2$ carbon, respectively. Calculating the neutron yield in CD_2 as function of initial deuteron energy from known cross sections⁹ and stopping powers,¹⁰ and assuming monoenergetic ions, yields a value of 500^{+100}_{-50} keV for the deuteron energy.

In order to determine that reflected neutrons were not being measured, the angular distribution of the neutron flux was studied and found consistent with the ion energy.

The total neutron yield in an experiment with 5-cm-diam CD_2 coating on the target and 4-cm-diam CD_2 coating on the anode was 5.7×10^9 . Under the assumption of monoenergetic ions of 500 keV this yields a total deuteron number of 3.6×10^{15} . Determination of the energy spectrum of the ions was not carried out. If a fraction of high-energy ions were responsible for a large fraction of the neutron yield, the total number of ions would be smaller than that determined by the assumption of a single energy. However, a significant number of ions in a high-energy tail of the spectrum would be incompatible with the relatively low neutron yield in the thick carbon target. A tail in the low-energy end of the spectrum would only cause the number of ions to be higher than our single-energy estimate. We therefore assume that a lower-limit estimate on the number of ions is obtained by taking the highest single energy compatible with the experimental errors. This yields a value of 2.4×10^{15} for the number of accelerated deuterons.

The net current in the drift tube was measured by two \dot{B} loops which were placed near the wall 7.5 and 36 cm from the anode. The traces are shown in Fig. 2. The loops were calibrated in the tube by discharging the machine into a conducting rod centered in the drift tube. The net beam current was due to electrons. Its magnitude was 42 kA in the nearer loop and 18 kA in the farther loop. The velocity of the beam front as determined from the two \dot{B} loop measurements was 0.7 cm/nsec, which is consistent with the velocity of 500 keV deuterons. The agreement between beam front velocity and ion velocity has been reported also in other configurations.¹¹ Some of the beam electrons were relativistic, as was evident from pin-hole photographs of metal targets placed in the beam.

The ion pulse width was inferred from the trace

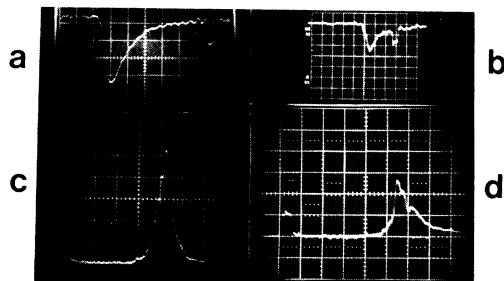


FIG. 2. (a) and (b), neutron detector signals. (a) Close detector; (b) far detector. Horizontal scale 50 nsec/div. (c) and (d), integrated \dot{B} loop signals. Horizontal scale 50 nsec/div. (c) Close loop, vertical scale 9.26 kA/div; (d) far loop, vertical scale 4.43 kA/div.

TABLE I. Relative neutron yield at a target distance of 4.5 cm from the anode.

d , diameter of CD ₂ coated area on anode (cm)	CD ₂ target diameter (cm)	Relative neutron yield
4.0	1.0	0.57
4.0	2.0	1.00
4.0	5.0	1.23
1.0	2.0	0.82
2.0	2.0	0.91
2.0 < d < 4.0	2.0	0.09

of the nearer fast-neutron detector (Fig. 2) placed 60 cm from the target. At this distance any energy dispersion in the neutrons could hardly affect the measured pulse width. We therefore take the width of the ion pulse on the target to be equal to the 50-nsec width of the neutron pulse. For the total deuteron number of 3.6×10^{15} this implies a deuteron current of 12 kA with total energy of 0.3 kJ.

The ion current density was studied by varying the CD₂-coated areas on both anode and target. When the diameter of the coated area on the target was reduced from 5 to 1 cm the ion current dropped only to 45% of the above, giving an ion current density of 5.8 kA/cm² at the center 1 cm diameter of the target. The divergence angle of the beam is demonstrated in Table I. The relative importance of the focal area of the pinch in ion generation is also demonstrated in the table. Out of the 4-cm-diam coated area on the anode 91% of the neutron counts from a 2-cm-diam target are by ions emitted from the center 2 cm diameter, and 82% by ions emitted from the center 1 cm diameter. In other experiments a 1-mm-thick aluminum anode was used with a 1-cm-diam, 40- μ m-thick aluminum window at the center, coated with CD₂. In these cases the neutron count was 65% of that in the case of a 4-cm-diam coating on a thin anode, again indicating the decisive role of the focal area. The ion pulse was delayed by 18 nsec relative to that of a thin anode, probably because of the difference in pinch dynamics between the two cases.

The ion generation and acceleration mechanisms are probably similar in principle, though not in detail, to those of the reflex diode. The space charge of the electrons in the focal region on the drift-tube side of the foil anode acceler-

ates the ions from the anode plasma. At the end of the acceleration stage these ions are neutralized by slow electrons and travel down the drift tube. The trajectories of the electrons forming the space charge are of course more complicated than those of the electrons in a planar reflex diode.

It is concluded from this work that the focal area of a tightly pinched relativistic electron beam can be used as a source of a high-current-density ion beam. Using this technique, ion current densities of several kiloamperes per square centimeter at several hundred kilovolts can be obtained even with such modest machines as ours.

¹M. J. Clauser, Phys. Rev. Lett. **35**, 848 (1975); J. W. Shearer, Nucl. Fusion **15**, 952 (1975).

²J. E. Graybill and J. R. Uglum, J. Appl. Phys. **41**, 236 (1970); J. Rander, B. Ecker, G. Yonas, and D. Drickey, Phys. Rev. Lett. **24**, 283 (1970).

³J. S. Luce, H. L. Sahlin, and T. H. Crites, IEEE Trans. Nucl. Sci. **20**, 336 (1973); G. W. Kuswa, Ann. N. Y. Acad. Sci. **251**, 514 (1975); D. W. Swain, G. W. Kuswa, J. W. Poukey, and C. R. Olson, in *Proceedings of the Ninth Conference on High Energy Accelerators, Stanford Linear Accelerator Center, Stanford, California, 1974*, CONF-740 522 (National Technical Information Service, Springfield, Va., 1974), p. 268; C. L. Olson, IEEE Trans. Nucl. Sci. **22**, 962 (1975); C. L. Olson, in *Proceedings of the Second Symposium on Ion Sources and Formation of Ion Beams, Berkeley, California, 1974* (Lawrence Berkeley Laboratory, Berkeley, Calif., 1974), p. III-3-1.

⁴S. Humphries, J. J. Lee, and R. N. Sudan, Appl. Phys. Lett. **25**, 20 (1974), and J. Appl. Phys. **46**, 187 (1975).

⁵J. M. Creedon, I. D. Smith, and D. S. Prono, Phys. Rev. Lett. **35**, 91 (1975); D. S. Prono, J. M. Creedon, I. Smith, and N. Bergstrom, J. Appl. Phys. **46**, 3310 (1975).

⁶J. W. Poukey, J. R. Freeman, M. J. Clauser, and G. Yonas, Phys. Rev. Lett. **35**, 1806 (1975); Shyke A. Goldstein and J. Guillory, Phys. Rev. Lett. **35**, 1160 (1975); J. Nation, J. Plasma Phys. **13**, 361 (1975).

⁷D. S. Prono, J. W. Shearer, and R. J. Briggs, Phys. Rev. Lett. **37**, 21 (1976).

⁸R. J. Lautner and D. E. Bannerman, Rev. Sci. Instrum. **39**, 1588 (1968).

⁹N. Jarmie and J. D. Seagrave, Los Alamos Scientific Laboratory Report No. LA2014, 1957 (unpublished).

¹⁰C. F. Williamson, J. P. Bonjot, and J. Picard, Centre d'Etudes Nucléaires, Scalay Report No. CEA R3042, 1966 (unpublished).

¹¹J. Rander, Phys. Rev. Lett. **25**, 893 (1970); B. Ecker, S. Putnam, and D. Drickey, IEEE Trans. Nucl. Sci. **20**, 301 (1973).

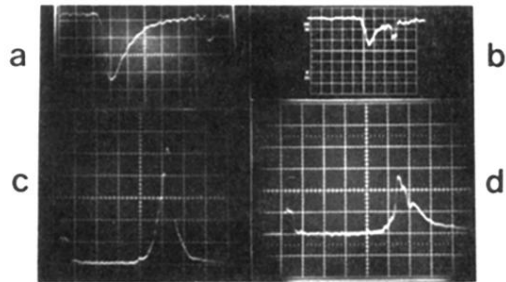


FIG. 2. (a) and (b), neutron detector signals. (a) Close detector; (b) far detector. Horizontal scale 50 nsec/div. (c) and (d), integrated \dot{B} loop signals. Horizontal scale 50 nsec/div. (c) Close loop, vertical scale 9.26 kA/div; (d) far loop, vertical scale 4.43 kA/div.